Fabrication and analysis of add-drop filters based on microring resonators in SiN

Tymon Barwicz, Milos A. Popovic, Peter T. Rakich, Michael R. Watts, Hermann A. Haus, Erich P. Ippen and Henry I. Smith

Research Laboratory of Electronics, Massachusetts Institute of Technology, 77 Massachusetts Ave, Cambridge, MA 02139 USA

tymon@mit.edu

Abstract: Add-drop filters based on microring resonators were fabricated in silicon-rich silicon nitride. Third-order microring filters showed an 80 GHz bandwidth, a 4 dB loss from input to drop, and a 24 nm free spectral-range.

OCIS codes: (230.3120) Integrated optics devices; (230.4000) Microstructure fabrication; (230.5750) Resonators

1. Introduction

High-index-contrast (HIC) microring resonators have been investigated for add-drop filters [1,2], lasers [3] and various non-linear switches [4]. HIC enables minute device sizes but causes difficulties in device fabrication due to strict requirements on dimensional control of submicron features. We report on the fabrication of first-, second-, and third-order series-coupled microring add-drop filters fabricated in silicon-rich silicon nitride (SiN). We describe the design, fabrication and characterization of the filters. Then, we compare measured and theoretically predicted filter responses. The third-order filters occupy an area of 50 by 15 μm. Although the filters employ the high index-contrast between SiN (n = 2.20) and air (n = 1), the third-order microring filters show a low 4 dB loss from input to drop. This is a 9 dB improvement over previously reported results on similar structures [2].

2. Design

Our objective was to design add/drop filters with a 40 GHz passband and a 24 nm free spectral-range (FSR) in the C-band. Sensitivity of resonance frequencies and bus-ring and ring-ring coupling to dimensional variations makes polarization-independent operation difficult to achieve in HIC. Therefore, we designed TE-only filters and rely on a scheme as in [5] for polarization independence.

To facilitate device fabrication, one approach would be to use lower index-contrast, which increases feature size and reduces scattering losses due to sidewall roughness. This approach was not employed in this paper, as it requires a reduced FSR to keep bending loss within acceptable bounds. While Vernier operation can be used to extend the FSR of a drop spectrum [6], it can introduce intolerable dispersion into thru-port channels.

A waveguide cross-section is shown in Fig. 1a. A single core layer of SiN on an SiO_2 cladding was used for bus waveguides and rings, with air top and side cladding. First-, second- and third-order filters were designed in a "series-coupled" microring configuration [1]. The rings were designed to support a high-Q fundamental TE mode (Q ~35k), but low-Q TM and higher-order TE resonant modes within the usable spectrum. Rings were chosen instead of racetrack resonators [2] as they have a higher uncoupled radiation Q for a given resonator path length, and do not suffer from scattering at bend-straight junctions. Using known synthesis techniques [1], higher-order filters were designed with a flat-top drop-port response. A simplified coupled-mode theory (CMT), based on that in the appendix of [1] but in 3D, was used to convert the desired power couplings to bus-ring and ring-ring spacings.

3. Fabrication

Fabrication of HIC microring resonators requires high-resolution lithography, strict dimensional control, and smooth sidewalls. Consequently, our fabrication process was based on direct-write scanning-electron-beam lithography (SEBL) and non-chemically-amplified resist. In addition, the fabrication process was optimized to reduce sidewall roughness using the scheme described in [7].

Silicon wafers where first thermally oxidized to form a 2.5-μm-layer of SiO_2. Then, a 315-nm-layer of SiN was deposited by low-pressure chemical-vapor-deposition (LPCVD) using a gas mixture of SiH_2Cl_2 and NH_3. SiN deposited in this way has low stress and low hydrogen-content. Hence, it exhibits low birefringence and negligible absorption in the telecommunication bands. This material is often called low-stress nitride. Next, 200 nm of poly-methyl-methacrylate (PMMA) and 40 nm of Aquasave were spun on. PMMA is a positive e-beam resist while Aquasave is a water-soluble conductive polymer from Mitsubishi Rayon used to prevent charging during SEBL. The

PMMA was exposed at 30 KeV using a Raith 150 SEBL system. The Aquasave was removed, and the PMMA developed. Next, 50 nm of Ni was evaporated on the structure, and a liftoff was performed by removing the non-exposed PMMA. Using the Ni as a hardmask, the waveguides where defined by conventional reactive-ion-etching (RIE). Vertical and smooth sidewalls where obtained with a gas mixture of CHF_3-O_2 in a 16:3 ratio. To obtain an accurate etch depth, the RIE was performed in several steps between which the etch depth was measured with a profilometer. Finally, the Ni was removed using a commercial wet Ni etchant.

This process has been shown to yield high resolution, accurate dimensional control, and smooth sidewalls. Ring-to-bus gaps as small as 50 nm were successfully fabricated. Strict dimensional control was confirmed by feature size measurements using the Raith 150 in scanning-electron-microscope (SEM) mode. High accuracy of the measurement was obtained by calibrating the deflection of the electron beam to the movement of the interferometric stage. During fabrication, the e-beam dose was selected to generate a correct bus waveguide width at the coupling region. This width was found to be accurate within the error of the measurement. However, as proximity effect corrections were not applied, repeatable width errors reaching 20 nm were observed on some 1050-nm-wide waveguides.

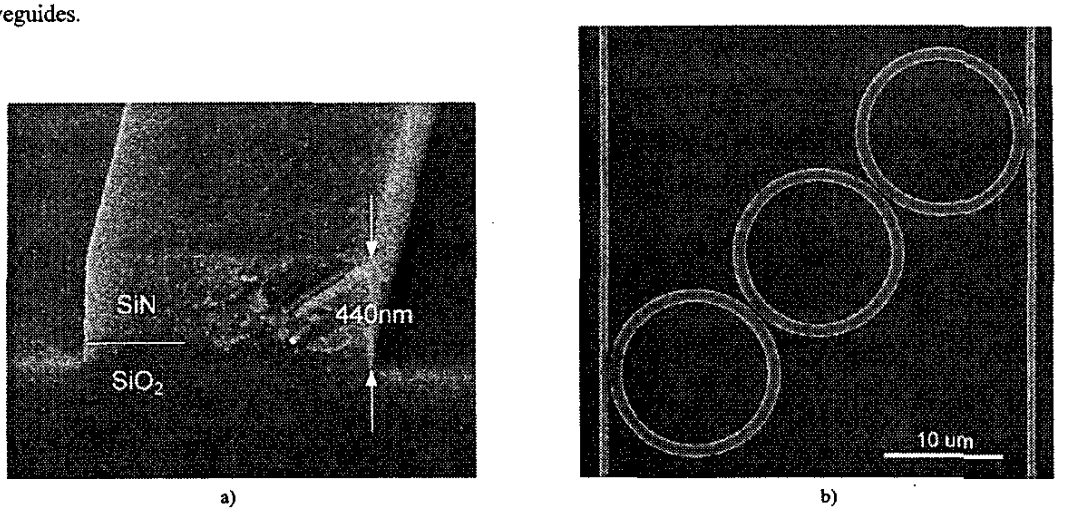

a) b)

Fig. 1 Micrographs of fabricated structures. a) Cross-section of a waveguide. The SiN layer is 315-nm-thick. Most of the waveguides were 1050-nm-wide. Some bus waveguides were 850 or 650-nm-wide for enhanced coupling to the rings. b) Third-order microring resonator. The rings outer radius is 7.3 μm.

4. Optical characterization

The devices were measured with a computer-controlled tunable laser, a Ge photodetector, and a lock-in amplifier. The laser was externally modulated with a chopper and coupled to the input facet of the waveguide with the use of both high-numerical-aperture-lens assemblies and lensed-fibers. The resulting guided mode was simultaneously imaged and detected through a non-dispersive microscope objective with an infrared vidicon camera and a large area Ge photodetector. The modulated optical signal was then electronically filtered with the lock-in amplifier and the transmission spectra acquired point by point as the laser wavelength was scanned with a computer interface. Great care was taken to ensure that the drop and through measurements were performed under similar conditions. To ensure a high degree of confidence, several measurements were repeated with two different collection methods. A measurement of the response of a third-order microring filter is presented in Fig 2.

Fabry-Perot loss measurements were performed on several straight waveguides. The measurements were consistent with a propagation loss of 3.6 dB/cm. An analysis based on mode overlaps indicated that the loss was mainly due to e-beam field-stitching errors. A rotational error in the field calibration created a 30 nm offset of the bus waveguides every 100 μm, which resulted in a loss of 0.021 dB/junction or 2.1 dB/cm.

5. Discussion

The large discrepancy between the observed 80 GHz and intended 40 GHz passband is attributed to error in the simple model used in the design process to translate desired coupling coefficients to physical gap distances. To understand the disagreement, 3D finite-difference time-domain (FDTD) simulations were used to calculate ring-bus and ring-ring coupling coefficients and coupler scattering losses in the post-fabrication analysis using measured dimensions and refractive indices. Vectorial CMT was used to predict the coupling-induced frequency shift [8].

These parameters, together with the ring mode propagation constant, were inserted into a scattering-matrix model for the filter (Fig. 2). Close agreement between theory and experiment is observed.

The expected microring bend-loss radiation Q was theoretically reduced to about 19,000 at the 1544 nm resonance due to a 5% thinner than expected core and 2% lower than expected vertical index-contrast. FDTD simulations indicate that additional losses were present in each of the rings due primarily to coupling to higher-order ring and radiation modes at the couplers. Since ring-bus coupler gaps are smaller than ring-ring coupler gaps, these losses reduced the Q of outer rings to about 9,500 and the Q of the central ring to about 13,000. Coupler scattering was found to be the dominant loss mechanism. With bending loss, it accounts for almost all observed loss.

Finally, the spectrum asymmetry, clearly visible in the thru response, is indicative of unequal resonance frequencies, with the central ring having a higher resonance frequency than the outer rings by about 22 GHz. This effect is explained by coupling-induced frequency shifting of resonators [8] due to the index perturbation caused by adjacent ring and bus waveguides. It limits the thru-port rejection to 8.5 dB in our experimental results, with a small discrepancy to theory.

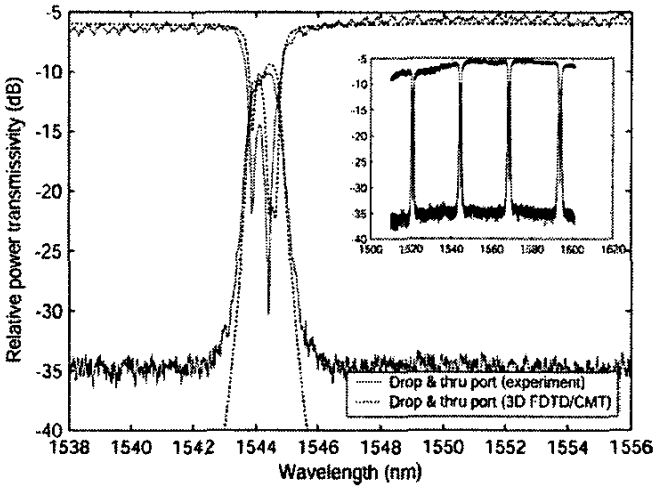

Fig. 2 Measured and theoretical spectral response of a third-order microring filter. The filter has an 80 GHz bandwidth, a 4 dB input-to-drop loss and a 24 nm FSR. The filter shows lower loss Q than expected, which is mainly due to scattering at the small ring-to-bus coupler gaps (60 nm). Coupling-induced frequency shifts are responsible for the asymmetry in the filter response.

6. Conclusion

We reported on the fabrication and characterization of SiN microring-resonator-based add-drop filters. A measured filter response was presented and compared with predicted results. Low filter loss and large FSR were obtained without employing the Vernier effect. Scattering at the ring-to-bus gaps and coupling-induced frequency shifts were found to degrade the filter response. A fabrication process yielding high resolution, accurate dimensional control and smooth waveguides was described. SiN has been shown to be a well-suited material for microring resonators.

7. References

1. B.E. Little, S.T. Chu, H.A. Haus, J.S. Foresi and J.-P. Laine, "Microring resonator channel dropping filters," J. Lightwave Technol. **15**, 998-1005 (1997).
2. J.V. Hryniewicz, P.P. Absil, B.E. Little, R.A. Wilson and P.-T. Ho, "Higher order filter response in coupled microring resonators," IEEE Photon. Technol. Lett. **12**, 320-322 (2000).
3. S. Park, S.S. Kim, L.W. Wang and S.T. Ho, "Single-mode lasing operation using a microring resonator as a wavelength selector", IEEE J. Quantum Electron. **38**, 270-273 (2002).
4. V. Van, T. A. Ibrahim, P. P. Absil, F. G. Johnson, R. Grover and P.-T. Ho," Optical signal processing using nonlinear semiconductor microring resonators", IEEE J. Quantum Electron. **8**, 705-713 (2002).
5. M. R. Watts, "Wavelength switching and routing through evanescently induced absorption," MS Thesis, Department of Electrical Engineering and Computer Science, Massachusetts Institute of Technology, Cambridge MA (2001).
6. Y. Yanagase, S. Suzuki, Y. Kokubun and S.T. Chu, "Box-Like Filter Response and Expansion of FSR by a Vertically Triple Coupled Microring Resonator Filter," J. Lightwave Technol. **20**, 1525-1529 (2002).
7. T. Barwicz and H.I Smith, "Evolution of line-edge-roughness during fabrication of high index-contrast microphotonic devices", submitted to the J. Vac. Sci. Technol. B.
8. C. Manolatou, M.A. Popovic, P.T. Rakich, T. Barwicz, H.A. Haus and E.P. Ippen, "Spectral anomalies due to coupling-induced frequency shifts in dielectric coupled resonator filters", *submitted concurrently to OFC 2004.*